A Highly Integrated MIMO Antenna Unit: Differential/Common Mode Design

Hang Xu, Steven Gao, *Fellow*, *IEEE*, Hai Zhou, Hanyang Wang, *Senior Member*, *IEEE*, and Yujian Cheng, *Senior Member*, *IEEE*

***Abstract*—A novel concept of antenna design, termed as differential/common mode (DM/CM) design, is proposed to achieve highly integrated multi-input multi-output (MIMO) antenna unit in mobile terminals. The inspiration comes from a dipole fed by a differential line which can be considered as a differential mode (DM) feed. What will happen if the DM feed is transformed into a common mode (CM) feed? Some interesting features are found in this research. By symmetrically placing one DM antenna and one CM antenna together, a DM/CM antenna can be achieved. Benefitting from the coupling cancellation of anti-phase currents and the different distributions of the radiation currents, a DM/CM antenna can obtain high isolation and complementary patterns, even if the radiators of the DM and CM antennas are overlapped. Therefore, good MIMO performance can be realized in a very compact volume. To validate the concept, a miniaturized DM/CM antenna unit is designed for mobile phones. 24.2 dB isolation and complementary patterns are achieved in the dimension of $0.330\lambda_0 \times 0.058\lambda_0 \times 0.019\lambda_0$ at 3.5 GHz. One 8×8 MIMO antenna array is constructed by using four DM/CM antenna units and shows good overall performance. The proposed concept of DM/CM design may also be promising for other applications that need high isolation between closely-packed antenna elements and wide-angle pattern coverage.**

***Index Terms*— Self-decoupled technique, mutual coupling, high isolation, mobile MIMO antenna, pattern diversity, complementary pattern, 5G communication.**

I. Introduction

As is well known, multi-input multi-output (MIMO) technology plays an important role in the 5th generation wireless systems (5G) [1-3]. However, it is still a great challenge for mobile terminals to achieve good MIMO performance. One of the reasons is that the limited space in mobile terminals restricts the amount of antenna elements of MIMO arrays and leads to poor isolation between antenna elements as well. Many scientists have spent a lot of efforts on the isolation problem.

The most popular idea of isolation enhancement may be introducing decoupling structures between antenna elements, including defected ground structure (DGS) [4], decoupling network [5], neutralization line [6], decoupling element [7], etc. There have been extensive applications of the aforementioned techniques [8-15]. Another way of isolation enhancement is utilizing the intrinsic high isolation between two antenna elements without any decoupling structure [16-23]; the combination of the two antennas and the corresponding high-isolation approaches could be named as MIMO antenna unit and self-decoupled technology respectively. The most famous self-decoupled technique should be orthogonal polarization, which has been widely used [16-20]. In addition, the reflection of high impedance area and the null area of electromagnetic energy could be used to achieve high isolation as well [21-23]. Self-decoupled technology has a unique advantage that no extra space is needed for any decoupling structure so the potential volume of MIMO antenna arrays could be more compact than the MIMO arrays with decoupling structures. However, the existing designs of MIMO antenna units usually need relatively large 2-dimentional (2D) area, which restricts their applications in mobile terminals.

In this paper, a novel concept of antenna design, termed as differential/common mode (DM/CM) design, is proposed to achieve highly integrated self-decoupled MIMO antenna unit in mobile terminals. The name 'DM/CM Design' refers to that a DM antenna and a CM antenna are symmetrically integrated to obtain a DM/CM antenna. Our research reveals that a DM/CM antenna could have intrinsic high isolation and complementary patterns even if the radiators of the DM antenna and the CM antenna are overlapped. Therefore, good MIMO performance can be realized in a very compact volume. To validate the concept, a miniaturized DM/CM antenna unit is designed for mobile phones. 24.2 dB isolation and complementary patterns are achieved in the dimension of $0.330\lambda_0 \times 0.058\lambda_0 \times 0.019\lambda_0$ at 3.5 GHz. One 8×8 MIMO antenna array is constructed by using four DM/CM antenna units and shows good overall performance.

II. Methodology of Differential/Common Mode Design

A. Principle of Differential/Common Mode Design

1) Evolution of Dipole

The idea comes from a dipole fed by a differential line, the

This work is funded by Huawei Technology Ltd (China), EPSRC grants EP/N032497/1, EP/P015840/1, and EP/S005625/1.

H. Xu and S. Gao are with the School of Engineering and Digital Arts, University of Kent, Canterbury, CT2 7NT, United Kingdom (e-mail: 54773906@qq.com and S.Gao@kent.ac.uk).

H. Zhou and H.Y. Wang are with Huawei Technology Ltd, 300 South Oak Way, Green Park, Reading RG2 6UF, Berkshire, United Kingdom (e-mail: Hanyang.Wang@huawei.com and Hai.Zhou1@huawei.com).

Y.J. Cheng is with the EHF Key Laboratory of Fundamental Science, School of Electronic Engineering, University of Electronic Science and Technology of China (UESTC), Chengdu 611731, China (e-mail: chengyujian@uestc.edu.cn).

current distributions of which are shown in Fig. 1(a). The solid black lines represent the currents of the dipole and the feed lines. The dashed black lines represent the pattern of the dipole in Plane XOY. From the current distributions, the vertical parts of Current 1 and Current 2 are very close to each other and anti-direction, so the radiation would cancel. Therefore, the main radiation current of the dipole is the horizontal parts of Current 1 and Current 2. Thus, the section pattern is 8-shape with two nulls at $\pm$X direction.

The feed of a differential line can be considered as differential mode (DM) feed. What will happen if the differential mode feed is transformed into common mode (CM) feed? The current distributions of the same dipole fed by CM are shown in Fig. 1(b). The solid blue lines represent the currents of the dipole and the feed lines. The dashed blue lines represent the pattern of the dipole in Plane XOY. Different from Fig. 1(a), the vertical parts of Current 3 and Current 4 are in the same direction, so the radiation would enhance and the section pattern is 8-shape with two nulls at $\pm$Y direction, which is similar to a dipole placed along Y-axis. The radiation pattern of horizontal parts of Current 3 and Current 4 also has two nulls at $\pm$ Y direction due to the cancellation of the anti-phase radiation. Therefore, the total radiation pattern in Plane XOY is a quasi-8-shape with two nulls at $\pm$ Y direction. The current distributions can be regarded as that a dipole placed along Y-axis is bent in the upper part as well.

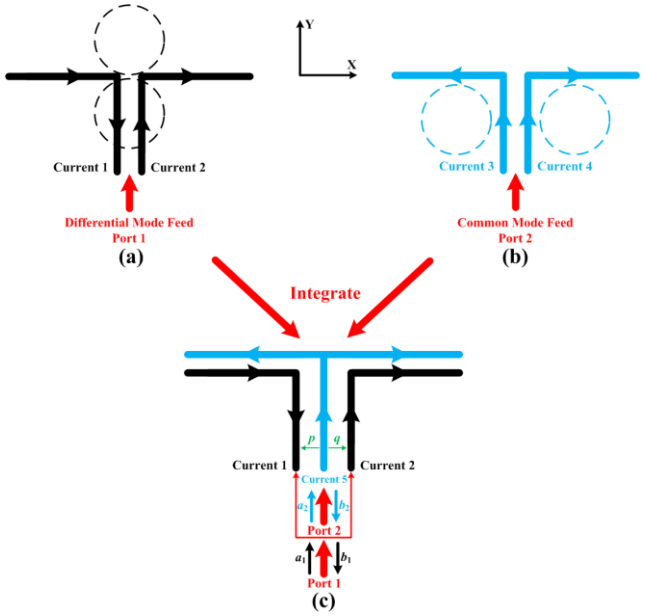

Fig. 1. Dipole fed by (a) differential mode and (b) common mode. (c) Integrated version.

2) Birth of DM/CM antenna

Compared Fig. 1(a) with Fig. 1(b), the patterns of the same dipole with the DM feed and the CM feed are complementary, especially that the angle of the maximum radiation of the DM antenna is exactly at the null of the CM antenna. As a result, the DM antenna and the CM antenna are integrated in Fig. 1(c) for the good space diversity which is important in MIMO technique. The combination of the DM antenna and the CM antenna is named as DM/CM antenna. The current distribution of the DM antenna is still represented by Current 1 and Current 2, while the current distribution of the CM antenna is equivalent to Current 5 of T-type since they have the same current route. The two-antenna system is considered as a two-port network to investigate the mutual coupling, i.e. S_{12} and S_{21}. We take S_{12} as the example here, since S_{21} is equal to S_{12} in terms of reciprocity theorem. In Fig. 1(c), a_1 and a_2 represents incident power waves, while b_1 and b_2 represents reflected power waves. According to the definition of S-parameters,

$$S_{12} = \frac{b_1}{a_2}|_{a_1=0} = \frac{b_1}{\text{const} \times I_{\text{Current 5}}}|_{a_1=0} \quad (1)$$

I_{Current5} is the equivalent magnitude of Current 5, and const (complex) is the ratio of a_2 and I_{Current5}. We assume that the current coupled from Current 5 to Current 1 (Current 2) and then outward from Port I is pI_{Current5} (qI_{Current5}); p and q are scalars and include the magnitude and the phase. Then, the total coupling b_1 can be written as

$$b_1 = pI_{\text{Current 5}} + qI_{\text{Current 5}}|_{a_1=0} \quad (2)$$

Bring equation (2) into equation (1),

$$S_{12} = \frac{pI_{\text{Current 5}} + qI_{\text{Current 5}}}{\text{const} \times I_{\text{Current 5}}} = \frac{p+q}{\text{const}} \quad (3)$$

In order to efficiently excite the antenna (large I_{Current5}), |const| should be as small as possible, so the only chance of reducing $|S_{12}|$ is the sum of p and q. It is easy to notice that Current 1 and Current 5 are in reverse direction, while Current 2 and Current 5 are in the same direction, so the value of p and q should partially cancel each other.

In order to achieve complete cancellation, Current 5 could be made self-symmetric and allocated in the center line of Current 1 and Current 2. Besides, the magnitude distributions of Current 1 and Current 2 should keep symmetric, so the coupling between Current 1 and Current 5 and the coupling between Current 2 and Current 5 have the same magnitude but anti-phase, i.e.

$$p = -q \quad (4)$$

Bring equations (4) into equation (3), we can obtain

$$S_{12} = S_{21} = 0 \quad (5)$$

Thus, in a DM/CM antenna, the mutual coupling between the DM antenna and the CM antenna could be very low, when 1) the distribution of current magnitude of the DM antenna is symmetric, and 2) the current distribution of the CM antenna is self-symmetric according to the axis of symmetry of the DM antenna. In short, symmetry is the key point of the design.

3) Demonstration Example

In order to demonstrate the concept of DM/CM design, a DM/CM antenna is shown in Fig. 2. Ant 1 is a dipole fed by a differential line the characteristic impedance of which is 250Ω. There is also a shunt capacitor (0.3 pF) at the open end of the differential line for reactance compensation. Obviously, Ant 1 is equivalent to the antenna with DM feed in Fig. 1(a). The antenna with CM feed in Fig. 1(b) is represented by Ant 2 which is a T-type dipole. The central lines of Ant 1 and Ant 2 are aligned. Besides, the layouts of Ant 1 and Ant 2 along X-axis are parallel and overlapped. There is a gap of 2 mm between Ant 1 and Ant 2 along Z-axis for proper arrangement. In order to demonstrate the principle in a stronger EM coupling environment, the horizontal parts (along X-axis) of Ant 2 are

This article has been accepted for publication in a future issue of this journal, but has not been fully edited. Content may change prior to final publication. Citation information: DOI 10.1109/TAP.2019.2922763, IEEE Transactions on Antennas and Propagation

made longer, so the radiation currents of Ant 1 and Ant 2 can be as close as possible, which means the absolute value of p and q is larger. The layouts of Ant 1 and Ant 2 have a uniform width of 1 mm.

From the simulated S-parameters in Fig. 3, Ant 1 and Ant 2 both resonate at 3.5 GHz. Although the layouts of Ant 1 and Ant 2 are extremely close, the isolation between Ant 1 and Ant 2 is >55 dB. The simulated current distributions of Ant 1 and Ant 2 at 3.5 GHz are shown in Fig. 4. It can be easily observed that the distributions agree well with the current model in Fig. 1(c). The feature of high isolation just benefits from the anti-phase cancellation of the coupling currents.

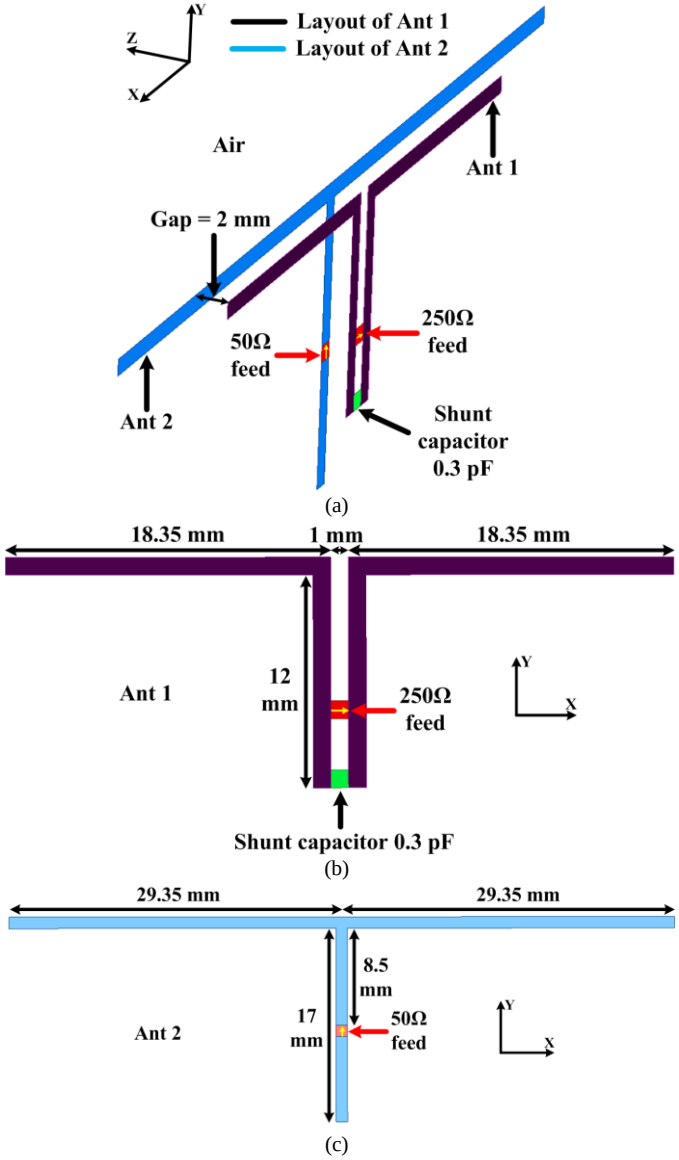

Fig. 2. Configuration of a DM/CM antenna. (a) Overall view. Detailed dimensions of (b) Ant 1 and (c) Ant 2.

The simulated 3-dimentional (3D) patterns are shown in Fig. 5. The pattern of Ant 1 is omnidirectional in Plane YOZ and has two nulls at ±X direction, while the pattern of Ant 2 covers the angles of the weak radiation of Ant 1. Therefore, the complementary coverage of 3D space is achieved, which benefits from the entirely different distributions of the radiation currents of Ant 1 and Ant 2. The 2D patterns in Plane XOY (Fig. 6(a)) are similar to the predicted patterns in Fig. 1(a)(b) and further demonstrate the feature of complementary patterns. From the 2D patterns in Plane YOZ (Fig. 6(b)), the radiation of Ant 1 and Ant 2 possesses different co-polarization and good level of cross-polarization (35.9 dB for Ant 1 and 19.6 dB for Ant 2), which is advantageous for the improvement of channel capacity.

This design example demonstrates the characteristics of high isolation and complementary patterns of DM/CM antenna in an ideal environment. Next, the proposed idea will be applied to mobile antennas.

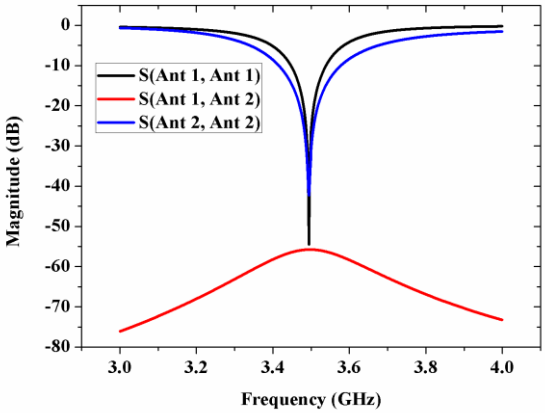

Fig. 3. Simulated S-parameters.

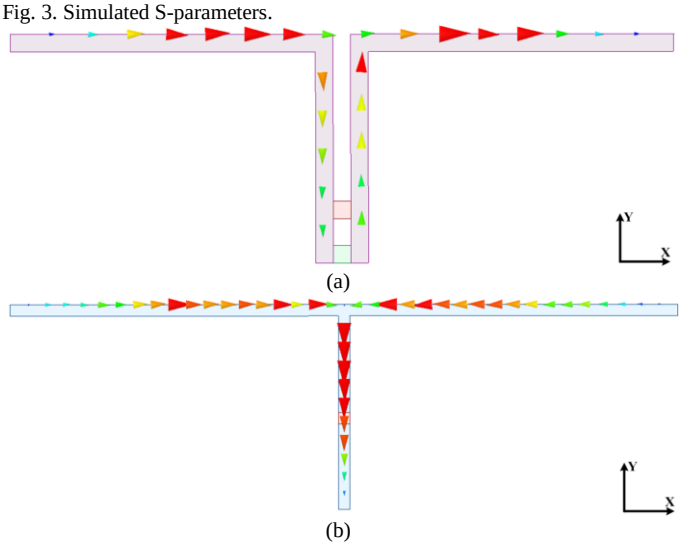

Fig. 4. Vector current distributions of (a) Ant 1 and (b) Ant 2 at 3.5 GHz.

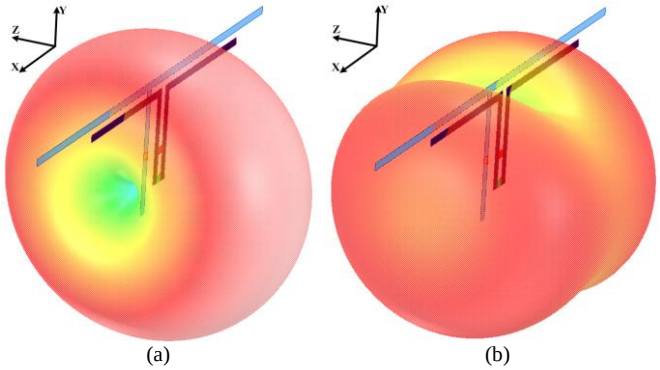

Fig. 5. 3D patterns of (a) Ant 1 and (b) Ant 2 at 3.5 GHz.

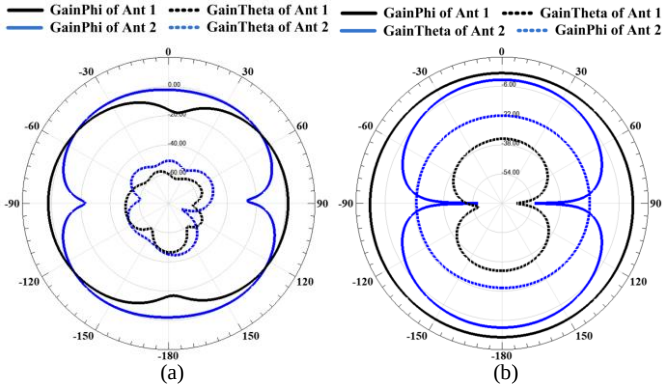

Fig. 6. 2D patterns of Ant 1 and Ant 2 at 3.5 GHz. (a) Plane XOY. (b) Plane YOZ.

B. Miniaturization Design of DM/CM Antenna

In terms of the principle of DM/CM design, even if the radiators of two antennas with DM feed and CM feed respectively are overlapped, good isolation and space diversity can still be achieved. However, the DM/CM antenna in Section II-A is still bulky for mobile phones, so miniaturization design is essential.

1) Differential Mode

In this research, the chosen radiator of the DM antenna is a dipole which resonates at $0.5\lambda_0$. The dipole in Fig. 2 is fed by a differential line which needs to be transformed into a microstrip line or a coaxial line by a balun, so the feed structures should consist of a balun transition and an impedance matching section, the dimension of which would be unacceptable in mobile phones. Therefore, a more compact feed is needed.

A Type-III balun is adopted to realize the transition between a coaxial line and the differential feed of a dipole [24]. In a traditional Type-III balun, the inner and outer conductors of a coaxial line act as the two resonant arms of a dipole respectively after the separation, and the outer conductor is also the metal ground. The key point of the balun is the symmetry, which is similar to the design of a DM/CM antenna. Different from a quarter-wavelength balun, Type-III balun is independent to the frequency, so it is promising for compact application.

A DM antenna with printed Type-III balun on the side-edge of a smart phone is designed in Fig. 7. In Fig. 7(a), there are three PCBs including Sub 1, Sub 2, and Sub 3. Sub 2 and Sub 3 have the same dimension of $134\times4.2\times1.6$ mm^3 and are perpendicularly placed on the two long edges of Sub 1 whose dimension is $150\times75\times0.8$ mm^3. There is a metal ground on the bottom layer of Sub 1 with the dimension of 134×71 mm^2, so the distance between the metal ground and the long edge of Sub 1 is 2 mm on each side. The DM antenna is in the middle of the long edge of the PCB. All the PCBs are FR4 (ε_r = 4.4, loss tangent = 0.02).

The configuration of the proposed DM antenna is shown in Fig. 7(b). Two symmetric Γ-strips with uniform width of 0.5 mm are used to act as the radiator of a dipole and part of a Type-III balun. The two strips are printed on one side of Sub 2 (close to +X direction, the other side is for the CM antenna) and connected to the metal ground of Sub 1. Part of the gap between the two Γ-strips (close to the metal ground) is filled with metal on the purpose of reactance compensation. Afterwards, a 50Ω coaxial line is attached to one Γ-strip. The inner and outer conductors of the coaxial line separate at the top of the strip, and then the inner conductor is connected to the other strip. The outer conductor of the coaxial line must be soldered to the strip and the metal ground to prevent another current path. Then, a revised Type-III balun is achieved. In fact, section ABCD is the radiator of the dipole and section BCEF is the printed Type-III balun.

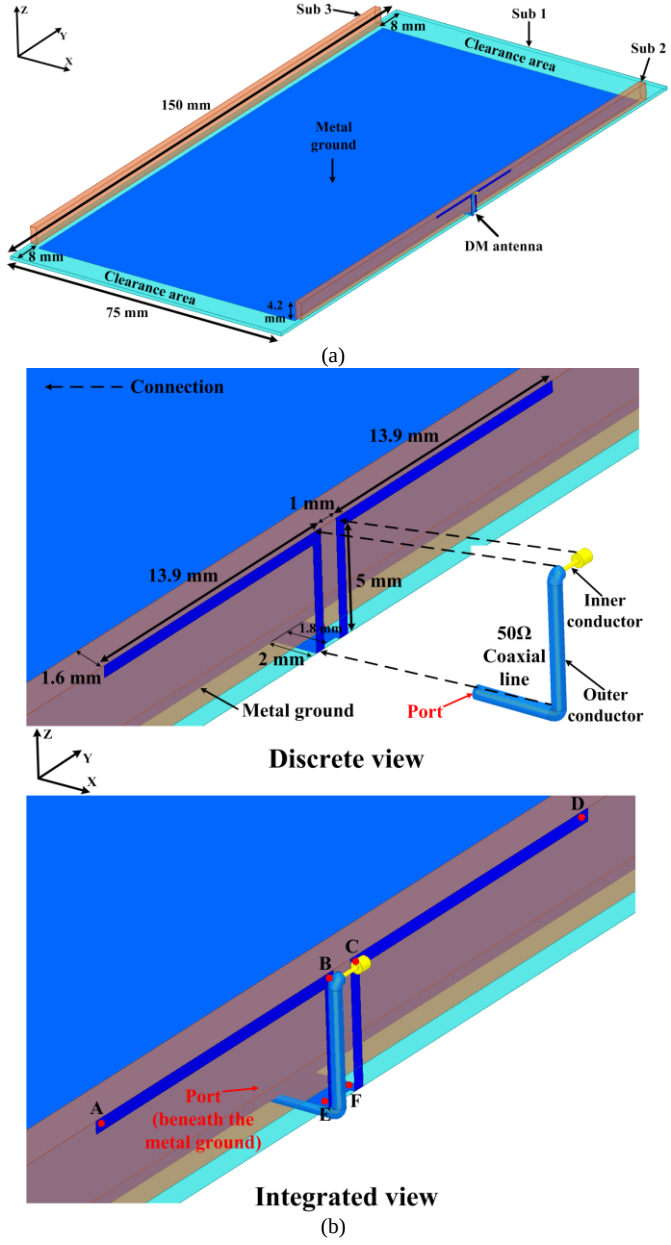

Fig. 7. A DM antenna on the side-edge of a smart phone. (a) Overall view. (b) Enlarged view.

2) Common Mode

Now, let us integrate the CM antenna into the DM antenna. In Fig. 2, the resonator of the CM antenna is a T-type dipole, which is difficult to achieve in low profile. Besides, its feed is harder to be transformed into a microstrip line or a coaxial line than that of the DM antenna. As a result, a T-type monopole is adopted on the purpose of miniaturization and convenient feed.

This article has been accepted for publication in a future issue of this journal, but has not been fully edited. Content may change prior to final publication. Citation information: DOI 10.1109/TAP.2019.2922763, IEEE Transactions on Antennas and Propagation

One resonant arm of the T-type monopole is a flat metal ground rather than a microstrip line, so the 3D pattern cannot be as regular as it is shown in Fig. 5(b) any more. However, the patterns of the DM antenna and the CM antenna are still complementary, which will be shown later. The other features of DM/CM antenna are reserved as well.

From the configuration in Fig. 8, the T-type monopole is printed on one side of Sub 2 (close to –X direction). Afterwards, the monopole is connected to a 50Ω microstrip line on the top layer of Sub 1, and the microstrip line is fed by a 50Ω coaxial line below the metal ground. In order to compensate the reactance of the impedance, two symmetric grounding microstrip lines are used to act as shunt inductors. The layout of the CM antenna has a uniform width of 0.5 mm except the 50Ω microstrip line. From the perspective of impedance matching, one grounding microstrip line is actually enough for reactance compensation, but the principle of DM/CM design requires a good symmetry, so the symmetric grounding microstrip lines are essential. What is more, the central lines of DM and CM antennas are aligned. Then, a DM/CM antenna is achieved and the configuration is shown in Fig. 8(b). The whole DM/CM antenna occupies the dimension of 28.3×5×1.6 mm^3.

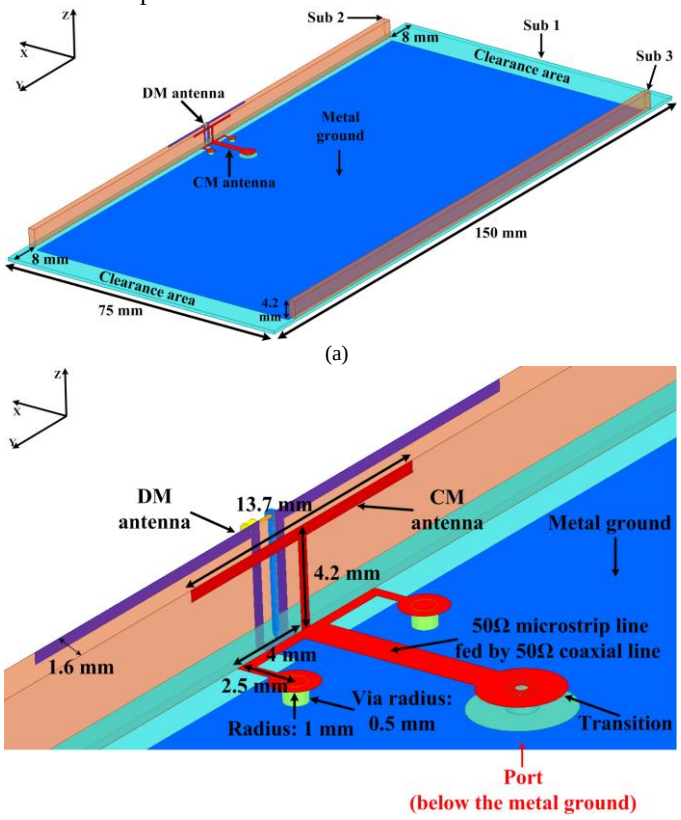

Fig. 8. A CM antenna is integrated into the DM antenna to obtain a DM/CM antenna. (a) Overall view. (b) Enlarged view.

3) Characteristics

The simulated S-parameters of the proposed DM/CM antenna are shown in Fig. 9. The -8 dB impedance bandwidth is 3.36-3.62 GHz for both the DM and CM antennas. The isolation between the DM antenna and the CM antenna is >31 dB. Compared with the result in Fig. 3, the isolation level decreases by 24 dB. The reason is that the symmetry of the DM antenna is affected by the nonideal balun, so the magnitude distribution of Current 1 and Current 2 (Fig. 1) has a little imbalance leading to tiny difference between the magnitude of p and q in equation (3), and thus S_{12} increases slightly. However, the isolation is still good.

In general, the price of good isolation is efficiency loss, because decoupling structures usually absorb EM energy. However, the proposed DM/CM antenna possesses intrinsic high isolation, so no extra decoupling structure is needed, which means no efficiency loss. In terms of the simulated antenna efficiency in Fig. 10, the DM and CM antennas have good total efficiency of >71% and >65% within 3.4-3.6 GHz respectively.

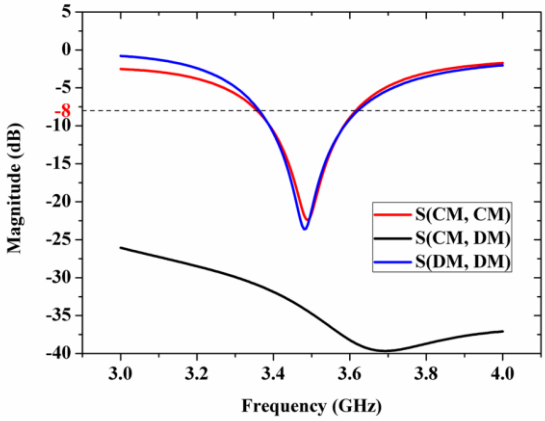

Fig. 9. Simulated S-parameters.

The simulated 3D patterns at 3.5 GHz are shown in Fig. 11. It can be clearly seen that the radiation of the DM antenna and the CM antenna covers different angles, especially that the radiation of the DM antenna covers the radiation null of the CM antenna at +X direction. In order to observe the feature of complementary patterns more clearly, 2D patterns are presented in Fig. 12. There is only total gain because the polarization is not pure due to the influence of the metal ground (travelling wave and standing wave). From the 2D patterns, it is interesting to see that most of the radiation null of the DM antenna is complemented by the radiation of the CM antenna, and vice versa.

The vector current distributions are shown in Fig. 13. The results demonstrate that: 1) the operating status of the DM/CM antenna agrees well with the current models in Fig. 1; 2) the revised Type-III balun successfully prevents the majority of the current from leaking to the feed structure; 3) the magnitude distribution of the current of the DM antenna has slight imbalance between the left Γ-strip and the right Γ-strip, which causes tiny mutual coupling between the DM and CM antennas.

The reflection coefficients of the DM antenna with and without the CM antenna are shown in Fig. 14. As is shown, the performance of the DM antenna has little variation. As a result, a researcher should design the DM antenna first and then the CM antenna. If the CM antenna is designed first, its performance would be influenced by the introduction of the DM antenna. It is because the metal ground is one resonant arm of the CM antenna, and the DM antenna is connected to the

metal ground, so the introduction of the DM antenna could change the operating status of the metal ground and then the CM antenna.

III. Characteristics of MIMO Antenna Array

A. Configuration

In Fig. 15, four identical DM/CM antenna units (same to the unit in Fig. 8) are symmetrically placed according to the center of Sub 1. The center-to-center distance between the antenna units on the same long edge of the PCB is set to be 92 mm for a good overall performance. There are two antennas in each DM/CM antenna unit, so an 8×8 side-edge MIMO antenna array is constructed. In the array, the performance of the DM antennas does not change much on account of the balanced feature, while the characteristics of the CM antennas are affected by the other antenna units and the change of the PCB ground.

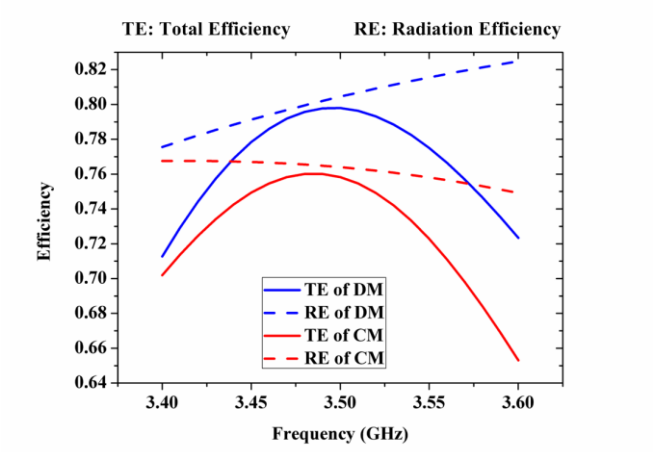

Fig. 10. Simulated antenna efficiency.

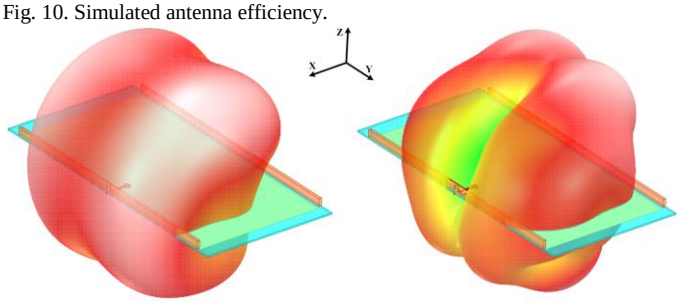

(a) (b)

Fig. 11. 3D patterns of (a) DM antenna and (b) CM antenna at 3.5 GHz.

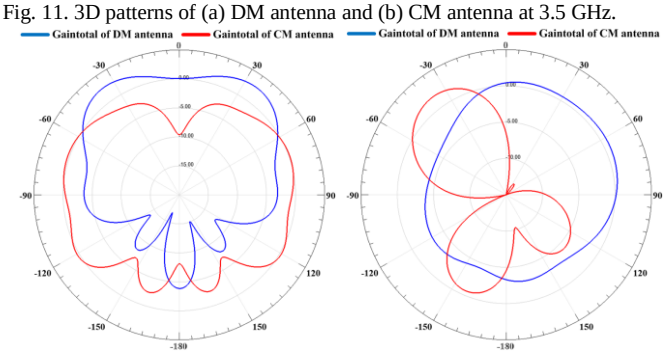

(a) (b)

Fig. 12. 2D patterns of DM and CM antennas at 3.5 GHz. (a) Plane XOY (φ = -180 °~180 °). (b) Plane XOZ (θ = -180 °~180 °).

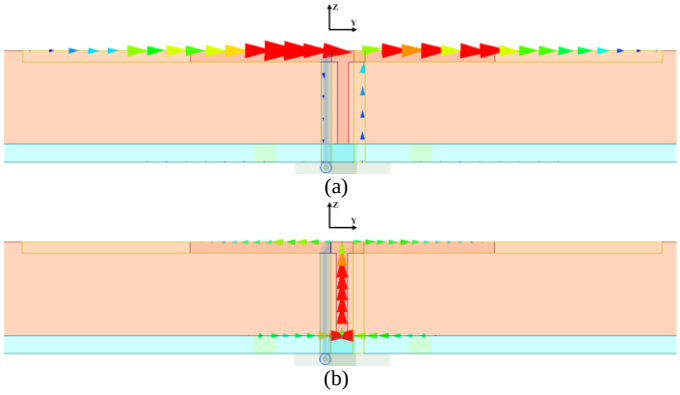

(a)

(b)

Fig. 13. Vector current distributions of (a) DM antenna and (b) CM antenna at 3.5 GHz.

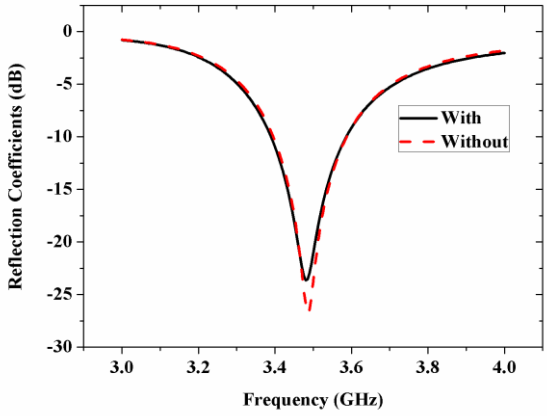

Fig. 14. Reflection coefficients of DM antenna with/without CM antenna.

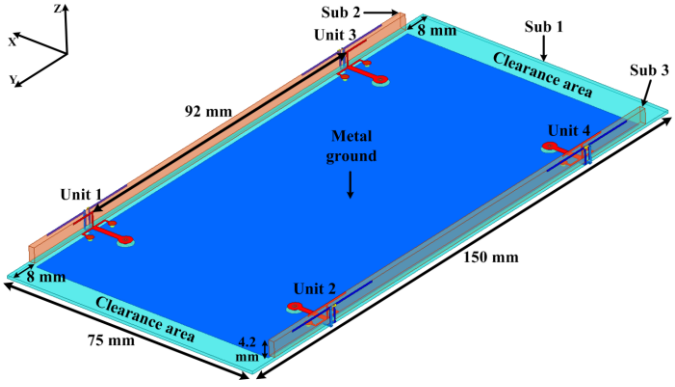

Fig. 15. Configuration of 8×8 side-edge MIMO antenna array.

B. Simulation

On account of the identity of the four antenna units, the simulated S-parameters and antenna efficiency are shown only for Unit 1. From Fig. 16, the -8 dB impedance bandwidth of Unit 1 is 3.37-3.61 GHz for the DM antenna and 3.35-3.63 GHz for the CM antenna. Compared with the results in Fig. 9, the bandwidth does not change much.

In Fig. 17, the mutual coupling between the DM antenna of Unit 1 and the other antennas (include the CM antenna of Unit 1) is presented. The isolation between the DM and CM antennas of Unit 1 is >30 dB which is similar to the result in Fig. 9, so the feature of intrinsic high isolation of DM/CM antenna is still available in antenna arrays. The isolation between the DM

antenna of Unit 1 and the other antenna units is >20 dB, which is good as well. From the results in Fig. 18, the mutual coupling between the CM antenna of Unit 1 and the other antenna units is >18 dB, which can be further improved with other decoupling techniques.

In Fig. 19, the radiation efficiency and total efficiency of Unit 1 are presented. In comparison with the results in Fig. 10, the total efficiency decreases from >71% to >65% for the DM antenna and from 65% to 61% for the CM antenna. However, the performance does not deteriorate much and the efficiency is still good. Although not shown, the simulated efficiency of HFSS and CST agrees well [25, 26].

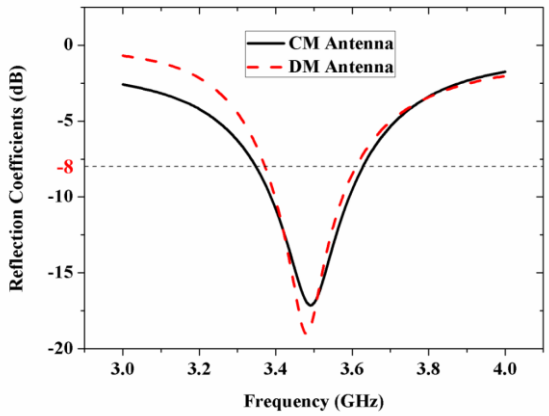

Fig. 16. Reflection coefficients of Unit 1.

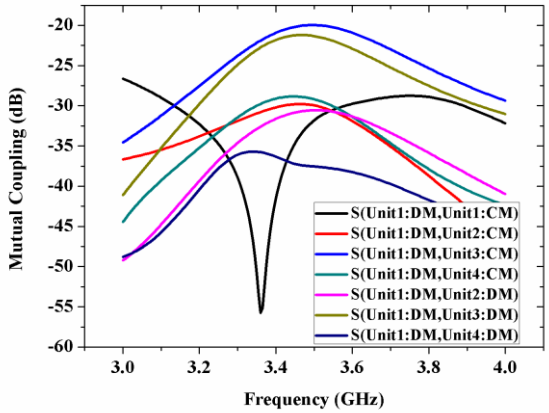

Fig. 17. Mutual coupling between the DM antenna of Unit 1 and the other antennas.

In order to demonstrate the pattern coverage of the 8×8 MIMO antenna array, 3D patterns of the eight antennas are shown in Fig. 20. Let us check the variation of the patterns of one antenna unit (Unit 1) first. Compared Fig. 20(a) with Fig. 11(a), more EM energy of the DM antenna is radiated to +Y direction, but the shape of the 3D pattern does not change much. Compared Fig. 20(b) with Fig. 11(b), the radiated EM energy of the CM antenna becomes more concentrated, which is caused by the change of the current distribution on the PCB.

From the eight pictures in Fig. 20, the feature of complementary patterns is still reserved for each antenna unit, but the patterns of some antennas have some overlapped coverage area such as the DM antenna of Unit 1 and the DM antenna of Unit 3. However, most EM energy of the DM antenna of Unit 1 is radiated to +Y direction, while that of the DM antenna of Unit 3 is radiated to –Y direction, so these two antennas still cover different angles. As a whole, the 8×8 MIMO antenna array possesses a good feature of pattern diversity.

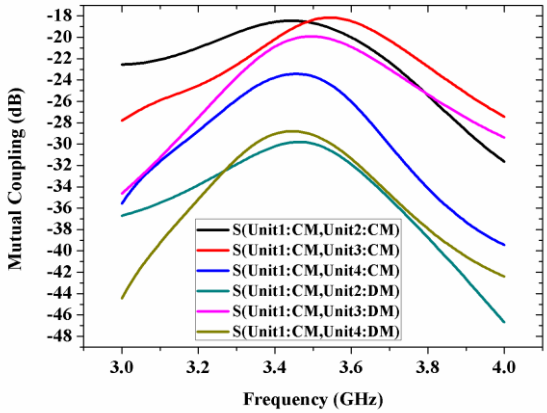

Fig. 18. Mutual coupling between the CM antenna of Unit 1 and the other antenna units.

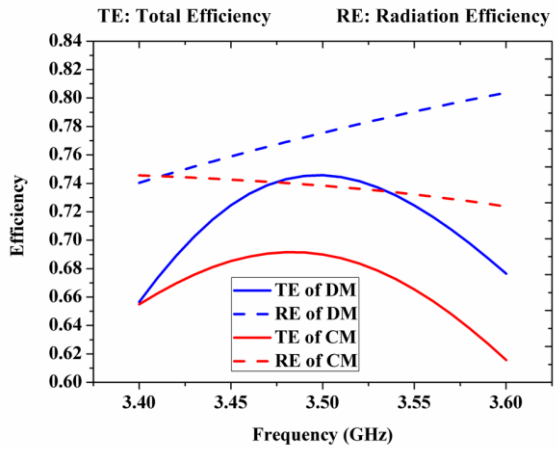

Fig. 19. Antenna efficiency of Unit 1.

C. Fabrication and Measurement

The 8×8 side-edge MIMO antenna array in Fig. 15 has been fabricated and measured. The prototype and the measured S-parameters are shown in Fig. 21 and Fig. 22 respectively.

In Fig. 22(a), the reflection coefficients of the eight antennas are shown. On account of the fabrication error, the resonant frequency of some antennas is not at 3.5 GHz but still close. The -8 dB impedance bandwidth of the DM antennas of the four antenna units is 180-220 MHz, which is narrower than the simulated result (240 MHz) in Fig. 16. However, the -8 dB impedance bandwidth of the CM antennas of the four antenna units is 270-300 MHz, which is wider than the simulated result (270 MHz) in Fig. 16. If -6 dB is chosen as the criteria, the bandwidth is wide enough to cover 3.4-3.6 GHz.

In Fig. 22(b), the mutual coupling between the DM and CM antennas of each antenna unit is presented. The isolation

is >24.1 dB for Unit 1, >24.2 dB for Unit 2, >21.6 dB for Unit 3, and >21.7 dB for Unit 4. Obviously, the measured results are 6.8-8.4 dB worse than the simulated results. The reason is that symmetry is the key point of high isolation, but it is difficult to achieve good symmetry in hand-made model. However, it should not be a problem if a mould is used in mass production. The measured isolation still demonstrates the practicability of the proposed principle.

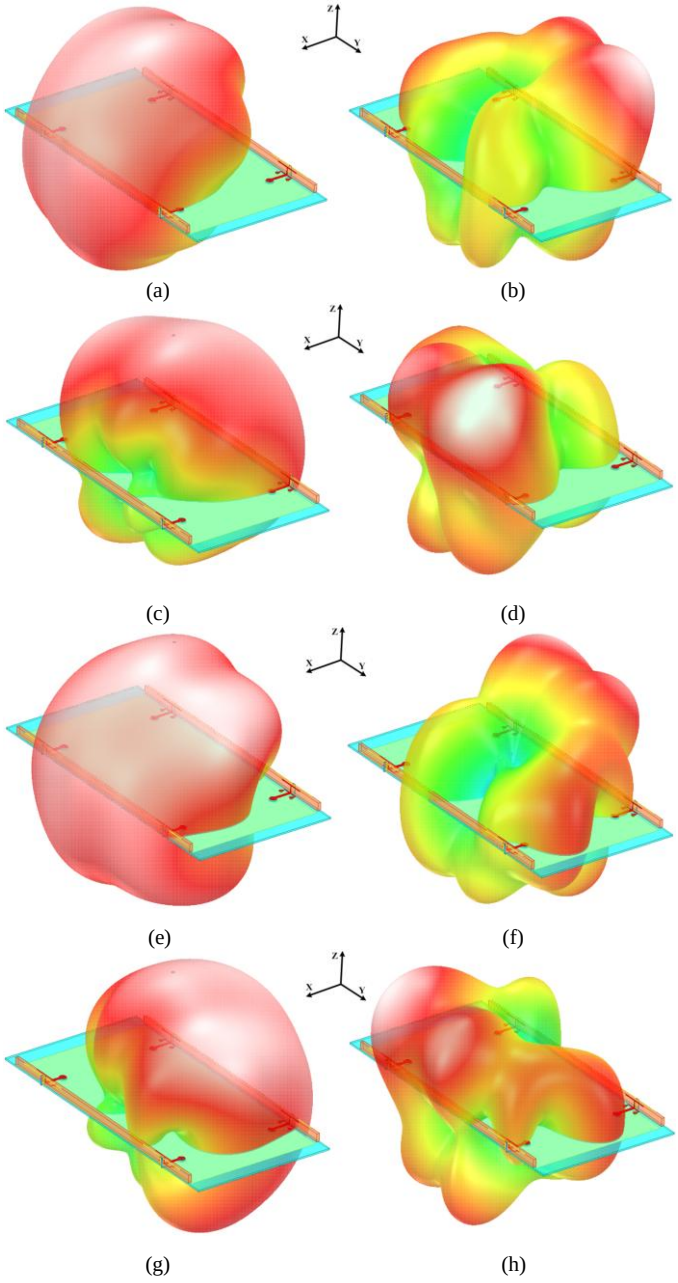

Fig. 20. Simulated 3D patterns of 8×8 MIMO antenna array. (a) DM antenna and (b) CM antenna of Unit 1. (c) DM antenna and (d) CM antenna of Unit 2. (e) DM antenna and (f) CM antenna of Unit 3. (g) DM antenna and (h) CM antenna of Unit 4.

For simplicity, only the mutual coupling between Unit 1 and the other antenna units is shown. In Fig. 22(c), the mutual coupling between the DM antenna of Unit 1 and the other antenna units is presented. The isolation is >21.8 dB which is good. In Fig. 22(d), the mutual coupling between the CM antenna of Unit 1 and the other antenna units is shown. The worst isolation is 15.7 dB, which is between the CM antennas of Unit 1 and Unit 3. The isolation of the other curves is still >18 dB. What should be mentioned is that the isolation between MIMO antenna units can be further enhanced with traditional decoupling techniques, about which there have been loads of papers.

Due to the lack of measurement equipment, we could only measure the 2D patterns rather than the 3D patterns. In Fig. 23, the measured results of Unit 3 at 3.5 GHz are shown. From Fig. 23(a), the weakest radiation of the CM antenna in Plane XOY is at around φ = 0°, while the supreme radiation of the DM antenna covers that angle range. In Plane XOZ (Fig. 23(b)), the weak radiation of the CM antenna is more obvious, but the radiation of the DM antenna could supplement the corresponding area as well. Therefore, the measured 2D patterns could still demonstrate the feature of complementary patterns of the proposed DM/CM antenna. In addition, the feature is quite stable within the operating frequency bands although not shown for simplicity. In Plane XOY, the measured peak gain of the DM antenna and the CM antenna is 6.00 dBi and 5.71 dBi respectively.

D. User's Hand Effect

The effect of a user's hand(s) on the antenna performance is investigated, which includes single-hand operation (SHO) and dual-hand operation (DHO), as is shown in Fig. 24(a). The antenna arrays at 3.5 GHz normally operate at data mode, so the effect of a user's head is not considered.

The simulated S-parameter and total efficiency are shown for SHO mode in Fig. 24(b)(c) respectively. Unit 1 is directly contacted by the hand, so the performance of its DM and CM antennas has the largest degradation: the reflection coefficients degrade dramatically, and the efficiency declines to < 10% due to the absorption effect of the hand. Unit 2 is not contacted but very close to the hand, so its efficiency is lower than Unit 3 and Unit 4. Although the hand influences symmetry of each DM/CM antenna unit, the isolation between the DM antenna and the CM antenna of each unit is still >21 dB; however, the good isolation of Unit 1 may be caused by the low antenna efficiency. The isolation between antenna units actually becomes better within 3.4-3.6 GHz (>21 dB, not shown for simplicity), because much EM energy has been absorbed.

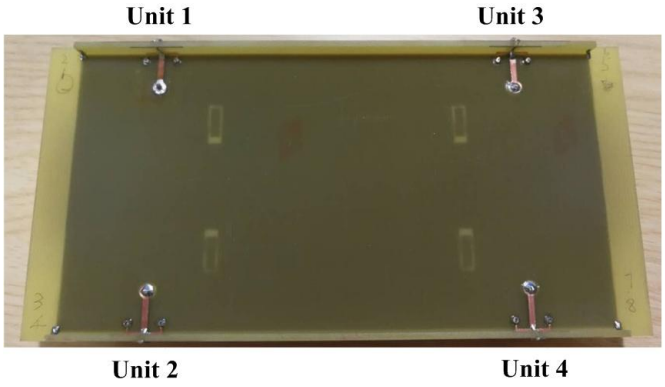

Fig. 21. Fabricated 8×8 MIMO antenna array.

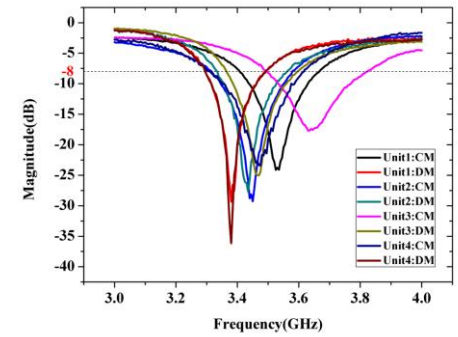

(a)

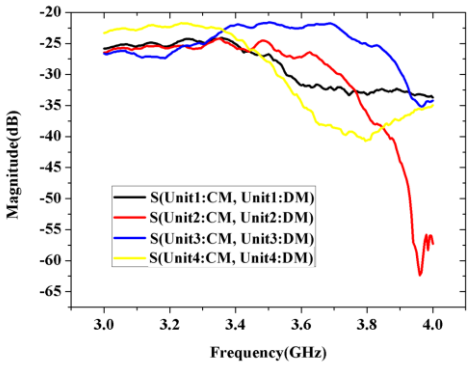

(b)

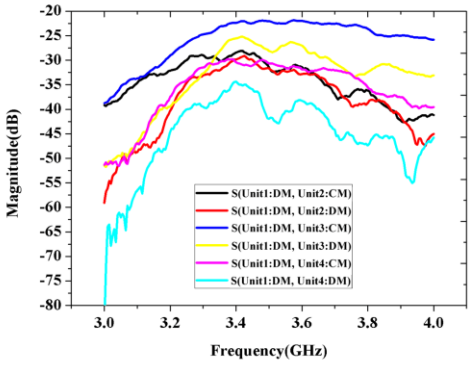

(c)

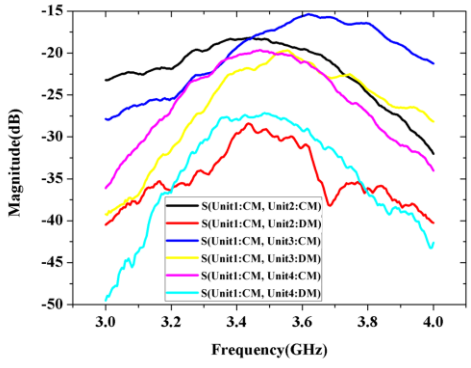

(d)

Fig. 22. Measured S-parameters. (a) Reflection coefficients. (b) Mutual coupling between the DM and CM antennas of each antenna unit. (c) Mutual coupling between the DM antenna of Unit 1 and the other antenna units. (d) Mutual coupling between the CM antenna of Unit 1 and the other antenna units.

The situation is better for DHO mode, because the hands do not contact the antennas directly. The configuration of the antennas with the hands is symmetric, so only the simulated S-parameter and total efficiency of Unit 1 and Unit 2 are shown in Fig. 24(d)(e) for simplicity. Obviously, the reflection coefficients do not deteriorate much, but the isolation between the DM antenna and the CM antenna of Unit 1 (Unit 2) decreases to 16.5 dB (18.4 dB) which is still acceptable. The isolation between antenna units is still good (>20 dB, not shown for simplicity)). The total efficiency of the CM antennas reduces to >38%, while that of the DM antennas remains >47%, because one resonant arm of the CM antennas (unbalanced antennas), i.e. the PCB ground, is partially covered by the hands, so the absorption effect is stronger.

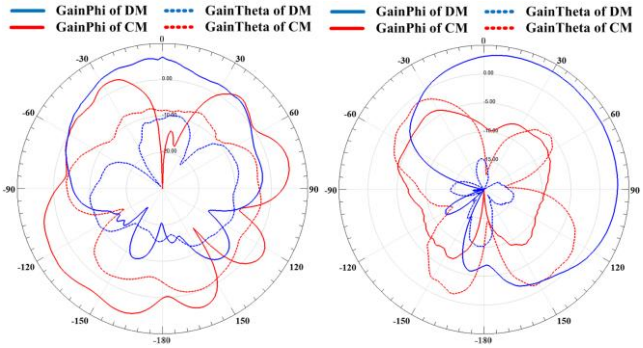

(a) (b)

Fig. 23. Measured 2D patterns of Unit 3 at 3.5 GHz. (a) Plane XOY (φ = -180 °~180 °). (b) Plane XOZ (θ = -180 °~180 °).

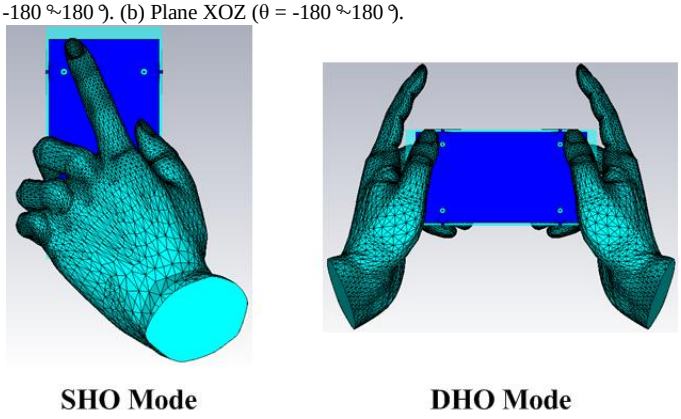

(a)

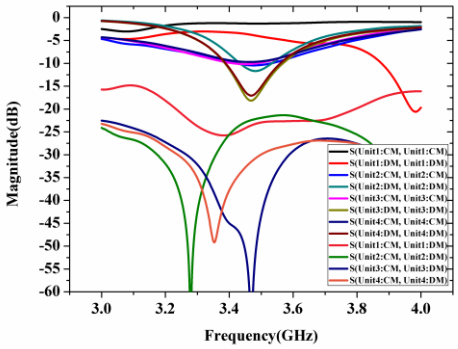

(b)

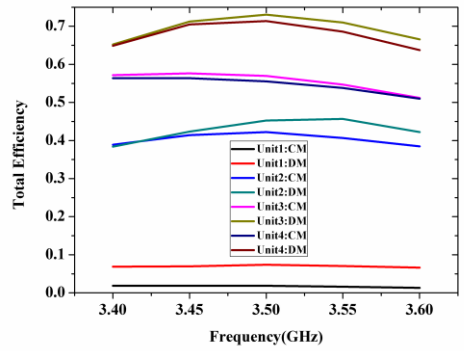

(c)

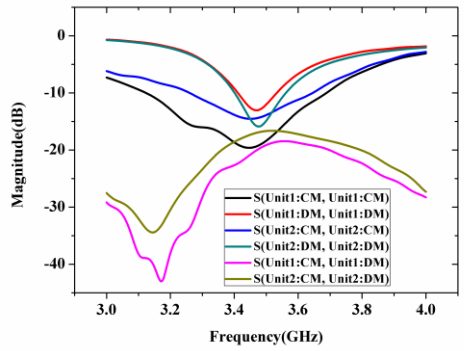

(d)

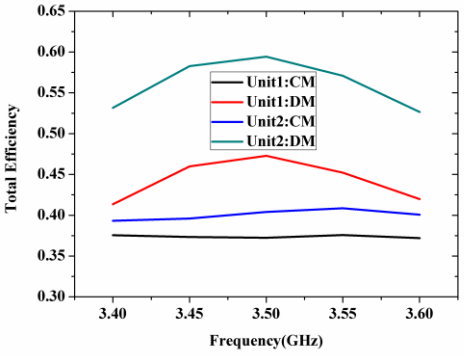

(e)

Fig. 24. The effect of a user's hand(s). (a) Two typical usage scenarios. (b) S-parameter and (c) total efficiency of the 8×8 MIMO antenna array at SHO mode. (d) S-parameter and (e) total efficiency of the 8×8 MIMO antenna array at DHO mode.

IV. Conclusion

In this paper, a novel concept of antenna design, namely DM/CM design, is proposed for achieving highly integrated MIMO antenna unit in mobile terminals. By utilizing the anti-phase cancellation of the coupling currents, high isolation can be achieved between two symmetrically placed antennas even if their radiators are overlapped. Another distinguished characteristic is the complementary patterns which benefit from the different distributions of the radiation currents. TABLE I shows a comparison between the proposed DM/CM antenna and other reported self-decoupled MIMO antenna units. Obviously, the design in this paper not only possesses high isolation and complementary patterns simultaneously but also significantly improves the integration level. A patent has been applied for the DM/CM antenna in Fig. 15[27]. Actually, a DM (CM) antenna could be any symmetric antenna fed by DM (CM), so a DM/CM antenna can consist of a variety of antennas. In addition, the proposed concept of DM/CM design may also be promising for other applications that need high isolation and wide-angle pattern coverage.

TABLE I
Comparison between Self-Decoupled MIMO Antenna Units

Ref.	Dimension (λ_0^3)	Bandwidth	Isolation (dB)	Complementary patterns
[19]	0.408× 0.408× 0.012	5.3%	35	Yes
[20]	0.269× 0.269× 0.026	4.9%	43	Yes
[21]	π*0.228× 0.228 ×0.026	3.7%	15	No
[22]	0.243× 0.182× 0.052	2.7%	20	No
[23]	0.212× 0.204× 0.061	7.7%	10	No
This paper	0.330× 0.058× 0.019	5.5%	24	Yes

References

[1] J.G. Andrews, et al, "What Will 5G Be?," *IEEE J. Sel. Areas Commun*, vol. 32, no. 6, pp. 1065-1082, Jun. 2014.

[2] V. Jungnickel, et al, "The Role of Small Cells, Coordinated Multipoint, and Massive MIMO in 5G," *IEEE Commun. Mag*., vol. 52, no. 5, pp. 44–51, May 2014.

[3] F. Boccardi, et al, "Five Disruptive Technology Directions for 5G," *IEEE Commun. Mag*., vol. 52, no. 2, pp. 74–80, Feb. 2014.

[4] C.-Y. Chiu, C.-H. Cheng, R. D. Murch, and C. R. Rowell, "Reduction of mutual coupling between closely-packed antenna elements," *IEEE Trans. Antennas Propag*., vol. 55, no. 6, pp. 1732–1738, Jun. 2007.

[5] S.-C. Chen, et al, "A decoupling technique for increasing the port isolation between two strongly coupled antennas," *IEEE Trans. Antennas Propag*., vol. 56, no. 12, pp. 3650–3658, Dec. 2008.

[6] A. Diallo, et al, "Study and reduction of the mutual coupling between two mobile phone PIFAs operating in the DCS 1800 and UMTS bands," *IEEE Trans. Antennas Propag*., vol. 54, no. 11, pp. 3063–3074, Nov. 2006.

[7] A.C. K.Mak, C. R. Rowell, and R.D. Murch, "Isolation enhancement between two closely packed antennas," *IEEE Trans. Antennas Propag*., vol. 56, no. 11, pp. 3411–3419, Nov. 2008.

[8] A. A. Al-Hadi, et al, "Eight-element antenna array for diversity and mimo mobile terminal in LTE 3500 MHz band," *Microw. Opt. Technol. Lett.*, vol. 56, no. 6, pp. 1323-1327, Jun. 2014.

[9] K.L. Wong and J.Y. Lu, "3.6-GHz 10-ANTENNA ARRAY FOR MIMO OPERATION IN THE SMARTPHONE," *Microw. Opt. Technol. Lett.*, vol. 57, no. 7, pp. 16991704, Jul. 2015.

[10] Y.L. Ban, et al, "4G/5G Multiple Antennas for Future Multi-Mode Smartphone Applications," *IEEE Access*, vol. 4, pp. 2981-2988, 2016.

[11] K.L. Wong, et al, "8-Antenna and 16-Antenna Arrays Using The Quad-Antenna Linear Array as A Building Block for The 3.5-GHz LTE MIMO Operation in The Smartphone," *Microw. Opt. Technol. Lett.*, vol. 58, no. 1, pp. 174-181, Jan. 2016.

[12] L.Y. Zhao and K.L. Wu, "A Dual-Band Coupled Resonator Decoupling Network for Two Coupled Antennas," *IEEE Trans. Antennas Propag.*, vol. 63, no. 7, pp. 2843–2850, Jul. 2015.

[13] Y. Wang and Z.W. Du, "A Wideband Printed Dual-Antenna With Three Neutralization Lines for Mobile Terminals," *IEEE Trans. Antennas Propag.*, vol. 62, no. 3, pp. 1495–1500, Mar. 2014.

[14] S. Zhang, Z. Ying, J. Xiong, and S. He, "Ultrawideband MIMO/Diversity Antennas with a Tree-Like Structure to Enhance Wideband Isolation," *IEEE Antennas Wireless Propag. Lett.*, vol. 8, pp.1279-1282, 2009.

[15] H. Xu, et al, "Multimode Decoupling Technique with Independent Tuning Characteristic for Mobile Terminals," *IEEE Trans. Antennas Propag.*, vol. 65, no. 12, pp. 6739–6751, Dec. 2017.
[16] S. Gao, et al, "A Broad-Band Dual-polarized Microstrip Patch Antenna with Aperture Coupling," *IEEE Trans. Antennas Propag.*, vol. 51, no. 4, pp. 898–900, Apr. 2003.
[17] M.Y. Li, Y.L. Ban, Z.Q. Xu, G. Wu, C.Y.D. Sim, K. Kang, and Z.F. Yu, "Eight-Port Orthogonally Dual-Polarized Antenna Array for 5G Smartphone Applications," *IEEE Trans. Antennas Propag.*, vol. 64, no. 9, pp. 3820-3830, Sep. 2016.
[18] M.Y. Li, Y.L. Ban, Z.Q. Xu, J.H. Guo, and Z.F. Yu, "Tri-Polarized 12-Antenna MIMO Array for Future 5G Smartphone Applications," *IEEE Access*, vol. 6, no. 1, pp. 6160-6170, Dec. 2017.
[19] W.W. Li, B. Zhang, J.H. Zhou, and B.Q. You, "High Isolation Dual-Port MIMO Antenna," *Electronics Letters*, vol. 49, no. 15, pp. 919-921, Jul. 2013.
[20] H. Wang, Z.J. Zhang, and Z.H. Feng, "Dual-Port Planar MIMO Antenna with Ultra-High Isolation and Orthogonal Radiation Patterns," *Electronics Letters*, vol. 51, no. 1, pp. 7-8, Jan. 2015.
[21] D.L. Wen, Y. Hao, M.O. Munoz, H.Y. Wang, and H. Zhou, "A Compact and Low-Profile MIMO Antenna Using a Miniature Circular High-Impedance Surface for Wearable Applications," *IEEE Trans. Antennas Propag.*, vol. 66, no. 1, pp. 96-104, Jan. 2018.
[22] S.C.K. Ko and R.D. Murch, "Compact Integrated Diversity Antenna for Wireless Communications," *IEEE Trans. Antennas Propag*., vol. 49, no. 6, pp. 954-960, Jun. 2001.
[23] Q.J. Rao and D. Wang, "A Compact Dual-Port Diversity Antenna for Long-Term Evolution Handheld Devices," *IEEE Trans. Vehicular Technology*, vol. 59, no. 3, pp. 1319-1329, Mar. 2010.
[24] John D. Kraus, Ronald J. Marhefka, Antennas: For All Applications, Third Edition, Asia: McGraw-Hill Education Co. and Publishing House of Electronics Industry, 2008, pp. 803–808.
[25] ANSYS HFSS. https://www.ansys.com/products/electronics/ansys-hfss
[26] CST Microwave Studio. https://www.cst.com/products/cstmws
[27] H. Xu, S. Gao, H. Zhou, and H.Y. Wang, A Common/Differential-Mode Antenna and Communication Products, Patent application number: PCT/CN2018/095709, filed Date: 13 July 2018 (China Patent, in Chinese).

Hang Xu received the Ph.D. degree from University of Kent, Canterbury, United Kingdom, in 2019.

His research interests include 5G smartphone antennas, MIMO antenna arrays, decoupling technology, microwave and millimeter-wave antennas, base station antennas.

Steven Shichang Gao (M'01-SM'16-F'19) received the PhD from Shanghai University, China.

He is a Full Professor and Chair in RF and Microwave Engineering, and the Director of Graduate Studies at the School of Engineering and Digital Arts, University of Kent, UK. His research covers smart antennas, phased arrays, MIMO, reconfigurable antennas, broadband/multiband antennas, satellite antennas, RF/microwave/mm-wave/THz circuits, mobile communications, satellite communications, UWB radars, synthetic-aperture radars, IOT and sensors for healthcare. He co-authored/co-edited three books (Space Antenna Handbook, Wiley, 2012; Circularly Polarized Antennas, IEEE-Wiley, 2014; Low-Cost Smart Antennas, Wiley, 2019), over 300 papers and 10 patents. He was a Distinguished Lecturer of IEEE AP Society, and is currently an Associate Editor of IEEE Transactions on Antennas and Propagation and several other international Journals (Radio Science, IEEE Access, Electronics Letters, IET Circuits, Devices and Systems, etc), and the Editor-in-Chief for John Wiley& Sons Book Series on "Microwave and Wireless Technologies".

He was General Chair of LAPC 2013, and an Invited Speaker at many conferences. He is a Fellow of IEEE, and also a Fellow of Royal Aeronautical Society, UK, and the IET, UK.

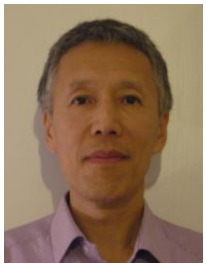

Hai Zhou received a Ph.D. degree on reflector antenna synthesis in 1987 from University of London, where he also carried out his post doctoral work until 1992.

He served as a senior lecturer at South Bank University, London before joining Lucent Technologies in 1996, working on GSM, UMTS and LTE in system engineering before joining Huawei Technologies in 2015. He worked on various topics from shaped reflector antenna synthesis, FDTD during his academic years to radio resource management and adaptive antennas in industry, with 18 patents, 14 journal papers and 34 conference papers. One of the papers won the Best Paper Award at the 19th European Microwave Conference in 1989, another received Oliver Lodge premium from IEE as the best paper of the year on Antennas and Propagation in 1991.

Hanyang Wang (SM'03) received the Ph.D. degree from Heriot-Watt University, Edinburgh, U.K. in 1995.

From 1986 to 1991, he served as a Lecturer and an Associate Professor with Shandong University, Jinan, China. From 1995 to 1999, he was a Post-Doctoral Research Fellow with the University of Birmingham, Birmingham, U.K., and the University of Essex, Colchester, U.K. From 1999 to 2000, he was with Vector Fields Ltd., Oxford, U.K., as a Software Development and Microwave Engineering Consultant Engineer. He joined Nokia U.K. Ltd., Farnborough, U.K. in 2001, where he had been a Mobile Antenna Specialist for 11 years. He joined Huawei Technologies after leaving Nokia, and he is currently the Chief Mobile Antenna Expert and the Head of the Mobile Antenna Technology Division. He is also an Adjunct Professor with the School of Electronics and Information Technology, Sichuan University, Chengdu, China. His current research interests include small and multi-band antennas for mobile terminals, antennas and antenna arrays for 5G mobile communications, and numerical methods for the solutions of electromagnetic radiation and scattering problems. He holds over 50 granted and pending US/EU/CN patents, and he has authored over 100 refereed papers on these topics.

He was a recipient of the Title of Nokia Inventor of the Year in 2005 and the Nokia Excellence Award in 2011. He was also a recipient of the Huawei Individual Gold Medal Award in 2012 and the Huawei Team Gold Medal Award in 2013 and 2014, respectively. His patent was ranked number one among 2015 Huawei top ten patent awards. Dr. Wang is a Huawei Fellow and an IET Fellow. He is an Associate Editor of the IEEE Antennas and Wireless Propagation Letters.

Yujian Cheng (SM'14) was born in Sichuan Province, China, on April, 1983. He received the B. S. degree from University of Electronic Science and Technology of China, in 2005 and the Ph.D. degree without going through the conventional Master's degree at Southeast University, Nanjing, China, in 2010.

Since 2010, he has been with the School of Electric Engineering, University of Electronic Science and Technology of China, and is currently a Professor. From 2012 to 2013, he was a research staff in the Department of Electrical and Computer Engineering, National University of Singapore. His current research interests include microwave and millimeter-wave antennas, arrays and circuits. He has authored or coauthored more than 100 papers in journals and conferences, as well as a book-Substrate Integrated Antennas and Arrays, (CRC press, 2015).

Dr. Cheng was the recipient of the National Science Fund for Excellent Young Scholars in 2016, Chang Jiang Scholars Program (Young Scholars) in 2016, the National Program for Support of Top-Notch Young Professionals in 2014, New Century Excellent Talents in University in 2013, and National Excellent Doctorate Dissertation of China in 2012. He is currently the secretary of the joint IEEE Chapters of APS/EMCS, Chengdu, China. He is the Senior Member of the Chinese Institute of Electronics. Now, Cheng has served as the Associate Editor for IEEE Antennas and Wireless Propagation Letters, and on review boards of various technical journals.